

A Novel Class of Potent Nonglycosidic and Nonpeptidic Pan-Selectin Inhibitors[§]

Holger K. Ulbrich,^{*,†,‡} Andreas Luxenburger,^{†,‡} Philip Prech,[†] Einar E. Eriksson,[#] Oliver Soehnlein,[#] Pierre Rotzius,[#] Lennart Lindbom,[#] and Gerd Dannhardt[†]

Department of Pharmaceutical and Medicinal Chemistry, Institute of Pharmacy, Johannes Gutenberg University, Staudingerweg 5, DE-55099 Mainz, Germany, and Department of Physiology and Pharmacology, Karolinska Institute, von Eulers väg 8, SE-171 77 Stockholm, Sweden

Received April 20, 2006

An early step of the inflammatory response, the rolling of leukocytes on activated endothelial cells, is mediated by selectin/carbohydrate interactions. The tetrasaccharide sialyl Lewis^x is a ligand for E-, P-, and L-selectin and therefore serves as a lead structure for the development of analogues. A combination of synthesis and structure-based design allowed rapid optimization. The current lead **2a** was evaluated in our E-selectin cell flow chamber assay where it proved to inhibit rolling and adhesion with an IC₅₀ of 28 ± 7 μM. The assays used are predictive for the in vivo efficacy of test compounds as shown for **2a** in a proteose peptone induced peritonitis model of acute inflammation in mice.

Introduction

Recruitment of circulating leukocytes from blood to tissue is an essential process in response to infection or tissue injury. However, excessive influx of leukocytes may result in adverse reactions that can be manifested in reperfusion injury, autoimmune diseases, and other acute or chronic disorders.^{1–4} The initial step in the inflammatory response is capture of leukocytes and their rolling along the endothelium in postcapillary venules.⁵ It has been shown that a set of inducible adhesion molecules, the so-called selectins, are critical in this process. They constitute a family of three structurally related calcium-dependent cell adhesion molecules that are expressed on the surface of activated vascular endothelial cells (E- and P-selectin), activated platelets (P-selectin), and leukocytes (L-selectin).⁶ To date, a number of natural selectin ligands have been identified.⁷ The common motifs recognized by all three selectins are the sialylated and fucosylated tetrasaccharide sialyl Lewis^x (sLe^x) (Figure 1) and sialyl Lewis^a (sLe^a), respectively.^{8,9} Thus, the ability to inhibit the recruitment of leukocytes by regulating interactions between the selectins and sLe^x or other ligands could have potential utility in a number of clinical diseases. Indeed, research on the design and synthesis of sLe^x mimetics has led to the development of a number of sugar- or nonsugar-based selectin inhibitors as well as related structures consisting of glycosylated peptides^{10–15} (Figure 1). Most of the inhibitors suffer from a lack of potency or poor pharmacokinetic properties and have often been difficult to synthesize. Nonetheless, the pan-selectin inhibitor bimosiamose (Revotar Biopharmaceuticals) has been effective in asthma, representing a proof of principle for selectin blockade in the treatment of inflammatory disease.¹⁶ Here, we describe the development of a novel benzoic acid type compound **1a** (Figure 1) with potent E-, P-, and L-selectin-blocking properties. This compound and closely related structures (Chart 1) represent new opportunities for the inhibition of selectin function in inflammation.

Molecular Modeling

A number of published studies have established key structural features of sLe^x necessary for binding to selectin proteins. The latest and most significant crystallographic experiments by Somers et al. involve solving the structure of sLe^x bound to E-selectin as well as P-selectin and the structure of the PSGL-1 N-terminus bound to P-selectin.⁸ The 3- and 4-hydroxy groups of the fucose moiety coordinate the calcium ion and interact additionally with further protein side chains. The 4-hydroxy functionality of galactose undergoes hydrogen bonding to the side chain of Tyr94, while the 6-OH group binds to the Glu92 side chain. The sialic acid interacts with the side chains of Arg97 and Tyr48 of E-selectin. This cocomplex of sLe^x and E-selectin is shown in Figure 2. The majority of the formed bonds within the binding pocket are of electrostatic nature. The buried surface area is relatively small with 549 Å².¹⁷ Previous molecular dynamics simulations¹⁸ of ligand/E-selectin complexes also suggested the existence of three essential binding sites of ligands for E-selectin as follows: (1) hydroxy groups coordinate to the calcium ion; (2) branched alkyl chains interfere with two hydrophobic regions on the surface of E-selectin; (3) a negatively charged group of the ligand interacts with the basic residues of E-selectin. These results gave rise to the synthesis of a variety of nonglycosidic and nonpeptidic low-molecular-weight selectin inhibitors in which the sugars in sLe^x have been substituted. The general outline that was previously published by Kondo and co-workers is shown in Figure 3a.¹⁸ On the basis of this pharmacophore model, our model consists of the following features (Figure 3b): (1) one of the carboxylic acids would coordinate to calcium; (2) the other at a distance of 8–9 Å is to form bonds by electrostatic interactions with Arg97 (E-selectin) or Lys99 in the case of P-selectin; (3) a long alkyl chain would interact with the shallow hydrophobic region consisting of Lys114, Ala9, Tyr49, etc. on E-selectin.⁸ The following results indicate that our pharmacophore model could have potential to find further selectin antagonists.

Ligand–E-selectin complexes were generated using the flexible docking procedure of the ICM (version 3.0) by Molsoft. Structural coordinates for the “receptor” were derived from the cocrystal structure of sLe^x and E-selectin from which the ligand was removed. Receptor grid maps were calculated with a grid spacing of 0.5 Å. The grid was defined in such a way that it

[§] Dedicated to Prof. Dr. Dr. Dres. h.c. E. Mutschler on the occasion of his 75th birthday.

* To whom correspondence should be addressed. Phone: +49 6131 39-24339. Fax: +49 6131 39-23062. E-mail: ulbrich@uni-mainz.de.

[†] Johannes Gutenberg University.

[‡] These authors contributed equally.

[#] Karolinska Institute.

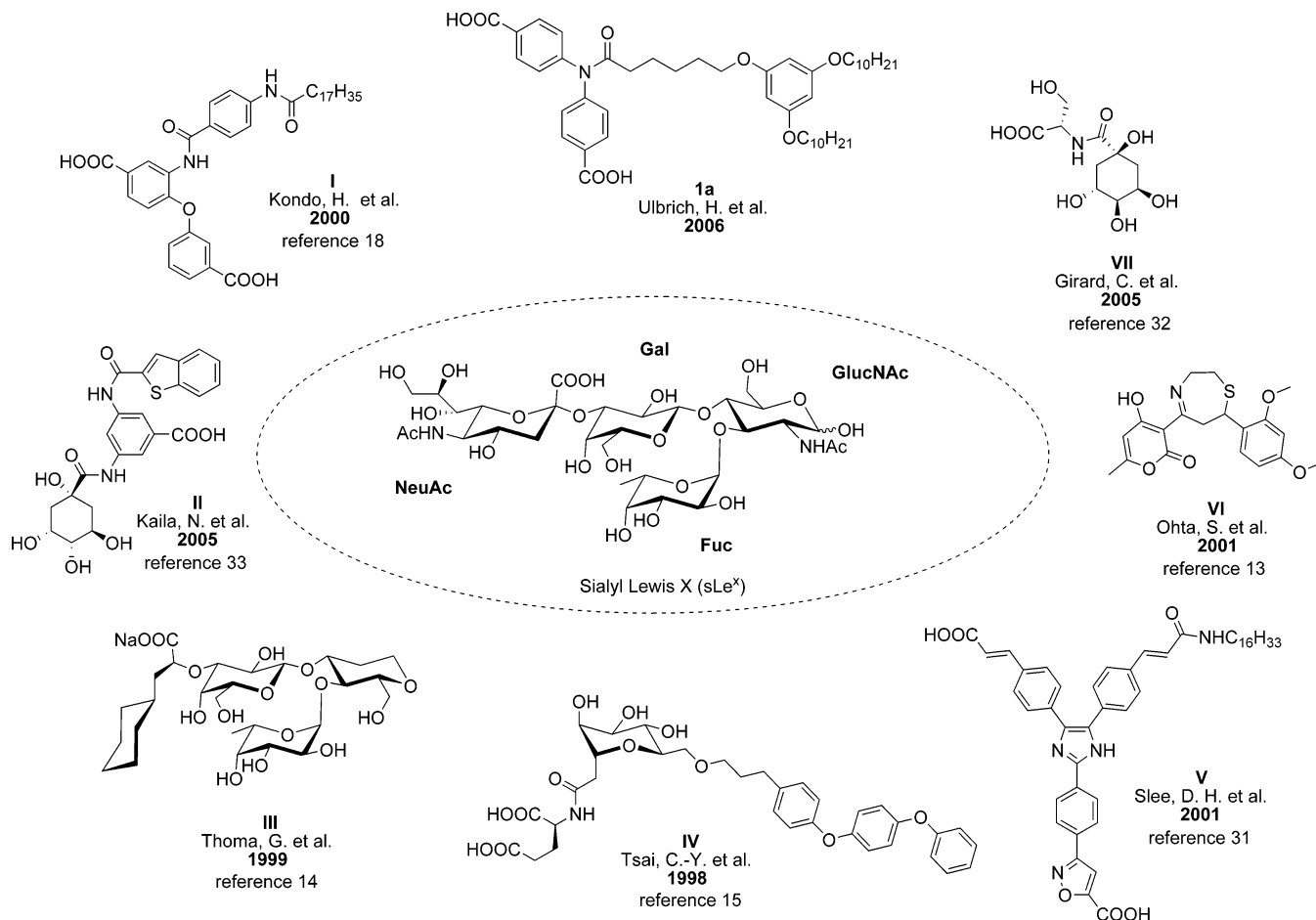


Figure 1. Representative chemical structures of some known selectin blockers.

included the ligand and key residues plus 3–5 Å in each of the *x*, *y*, *z* directions. For the ligands, 2D to 3D conversion is followed by energy minimization using the MMFF option as a force field. The docking algorithm implemented in ICM (version 3.0) optimizes the entire ligand in the receptor field, using a multistart Monte Carlo minimization procedure in internal coordinate space.

Chemistry

According to our molecular modeling considerations, we focused our synthesis on connecting the envisaged dicarboxylic acid functionalities with different types of spacer scaffolds.

Our approach toward the dicarboxylic acids **1a–c** (Figure 4) started from compounds **6a–c**, which were initially prepared by a Goldberg coupling reaction following the procedure described in ref 19 (Scheme 1a). Subsequent cleavage of the acetyl group combined with transesterification by refluxing **6a–c** in the presence of sodium methoxide in methanol provided the required diphenylamine building blocks **7a–c**. As the coupling products **6a–c** and thus the desired compounds **7a–c** as well were only obtained in moderate yields, we also became interested in looking into several other methods reported in the literature.^{20–22} When the copper-catalyzed methodology reported by Buchwald and co-workers²² was employed, the overall yields for the preparation of **7a** and **7b** improved significantly from 40–50% to 76–78% for the two steps.


The phenylbenzylamine precursors **7d–e** required for the synthesis of the dicarboxylic acids **1d–g** (Figure 4) were obtained from the condensation of 4-formylbenzoic acid methyl ester **8** and the aminobenzoic acid methyl esters **9a,b** to give

the corresponding imines **10a,b**, which were then treated with NaBH₄ in methanol at room temperature to give the desired amines **7d–e** in good yields.²³

Subsequent deprotonation of the amines **7a–e** with sodium hydride in *n*-Bu₂O and further reaction with 6-bromohexanoyl chloride gave rise to compounds **11a–e** (Scheme 1b).²⁴ To synthesize the phenolic coupling partners **15** and **18**, we etherified phloroglucin **14** in 1-decanol in the presence of HCl gas to produce 3,5-didecyloxyphenol **15**,²⁵ and resorcinol **17** was converted to 3-decyloxyphenol **18**²⁶ by treatment of **17** with potassium hydroxide in the presence of 1-bromodecane (Scheme 2). Compounds **11a–e** were then refluxed with **15** or **18** in the presence of potassium carbonate and a catalytic amount of potassium iodide or TBAI in cyclohexanone to achieve the desired coupling products **13a–g**. Saponification by stirring **13a–g** with a 0.5 M aqueous lithium hydroxide solution in THF accomplished the dicarboxylic acids **1a–g** (parts a and b of Scheme 1).

The preparation of the target dicarboxylic acids **2a,b** (Figure 4) began with a borane reduction of the amide function in **11a** and **11d** (Scheme 3).²⁷ The resulting amines **20a,b** were subsequently coupled with didecyloxyphenol **15**, applying the same reaction conditions as for the synthesis of compounds **13a–g** so that **21a,b** were isolated in good yields. Final saponification with potassium hydroxide accomplished the dicarboxylic acids **2a,b** in good yields.

The synthesis of the dicarboxylic acids **3a–c** (Figure 4) started from the iodide methyl esters **4b,c**, which were treated with *i*-PrMgCl at low temperatures (Scheme 4). In a halogen magnesium exchange reaction²⁸ the corresponding organomag-

Chart 1. Chemical Structures of the Investigated Compounds Representing Three Structural Classes: Amides (**1a–g** and **13a–g**), Amines (**2a,b** and **21a,b**), and Oximes (**3a–c** and **25a–c**)


	R ¹	R ²	R ³	E	n
1a	H	COOH	O(CH ₂) ₉ CH ₃	H	0
1b	COOH	H	O(CH ₂) ₉ CH ₃	H	0
1c	COOH	COOH	O(CH ₂) ₉ CH ₃	H	0
1d	H	COOH	O(CH ₂) ₉ CH ₃	H	1
1e	COOH	H	O(CH ₂) ₉ CH ₃	H	1
1f	H	COOH	H	H	1
1g	COOH	H	H	H	1
13a	H	COOMe	O(CH ₂) ₉ CH ₃	Me	0
13b	COOMe	H	O(CH ₂) ₉ CH ₃	Me	0
13c	COOMe	COOMe	O(CH ₂) ₉ CH ₃	Me	0
13d	H	COOMe	O(CH ₂) ₉ CH ₃	Me	1
13e	COOMe	H	O(CH ₂) ₉ CH ₃	Me	1
13f	H	COOMe	H	Me	1
13g	COOMe	H	H	Me	1

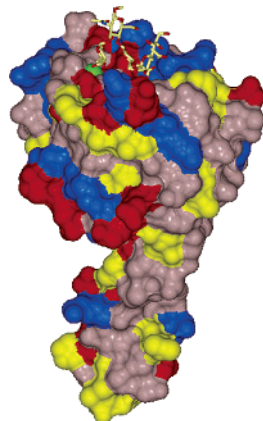
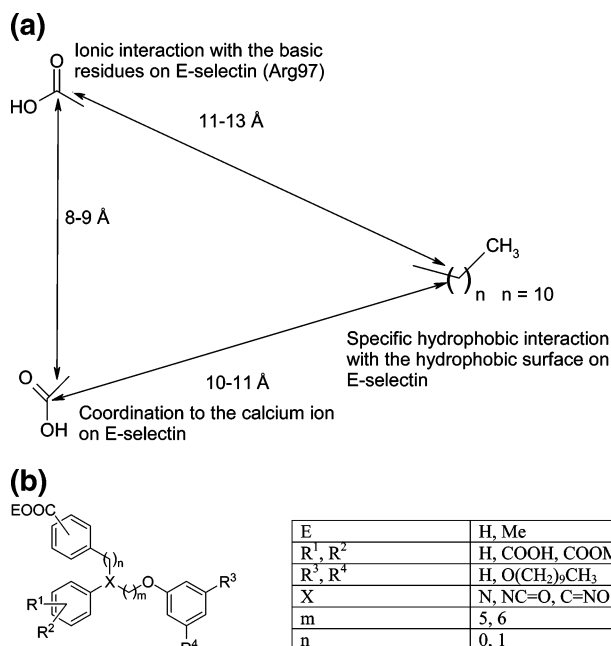
	R ¹	R ²	R ³	E	n
2a	H	COOH	O(CH ₂) ₉ CH ₃	H	0
2b	H	COOH	O(CH ₂) ₉ CH ₃	H	1
21a	H	COOMe	O(CH ₂) ₉ CH ₃	Me	0
21b	H	COOMe	O(CH ₂) ₉ CH ₃	Me	1

	R ¹	R ²	R ³	E
3a	H	COOH	O(CH ₂) ₉ CH ₃	H
3b	COOH	H	O(CH ₂) ₉ CH ₃	H
3c	H	COOH	H	H
25a	H	COOMe	O(CH ₂) ₉ CH ₃	Me
25b	COOMe	H	O(CH ₂) ₉ CH ₃	Me
25c	H	COOMe	H	Me

nesium intermediates were generated and reacted further with 4-formylbenzoic acid methyl ester **8** to provide alcohols **22a,b** in good yields. PCC oxidation led to the benzophenone derivatives **23a,b**, which were converted into the desired oximes **24a,b** by refluxing in ethanol in the presence of hydroxylamine hydrochloride and sodium acetate in good yields over two steps. **24b** was isolated as an inseparable mixture of *Z/E* isomers, and the ratio was determined to be 1:5 from the proton NMR spectrum. The required coupling partners **16** and **19** were obtained by additional etherification of **15** and **18** with 1,6-dibromohexane (Scheme 2). Compounds **24a,b** were then both coupled with **16** and **24a** additionally with **19** by deprotonating the oximes **24a,b** with sodium hydride in DMF and adding the corresponding bromide **16** or **19** together with a catalytic amount of TBAI at room temperature. Thus, the dimethyl esters **25a–c** were isolated in good yields. Finally, **25a–c** were saponified

by stirring with a 0.5 M aqueous sodium hydroxide solution in a mixture of ethanol and THF to provide the desired dicarboxylic acids **3a–c** in good yields.

The dichloro compound **28** was prepared from commercially available 4,4'-dichlorobenzophenone **26** (Scheme 5), which was readily converted into the corresponding oxime **27** by employing the same reaction conditions as for the synthesis of **24a,b**.

**Figure 2.** Crystal structure of sLe^x bound to the lectin domain of E-selectin. The bound calcium ion is represented by a green sphere, and sLe^x is shown in a capped stick model.⁸**Figure 3.** (a) From molecular modeling investigations by Kondo et al.,¹⁸ three critical interactions of ligands toward E-selectin were clarified. (b) Pharmacophore model that conserves the three essential groups to the desirable positions for E-selectin binding.

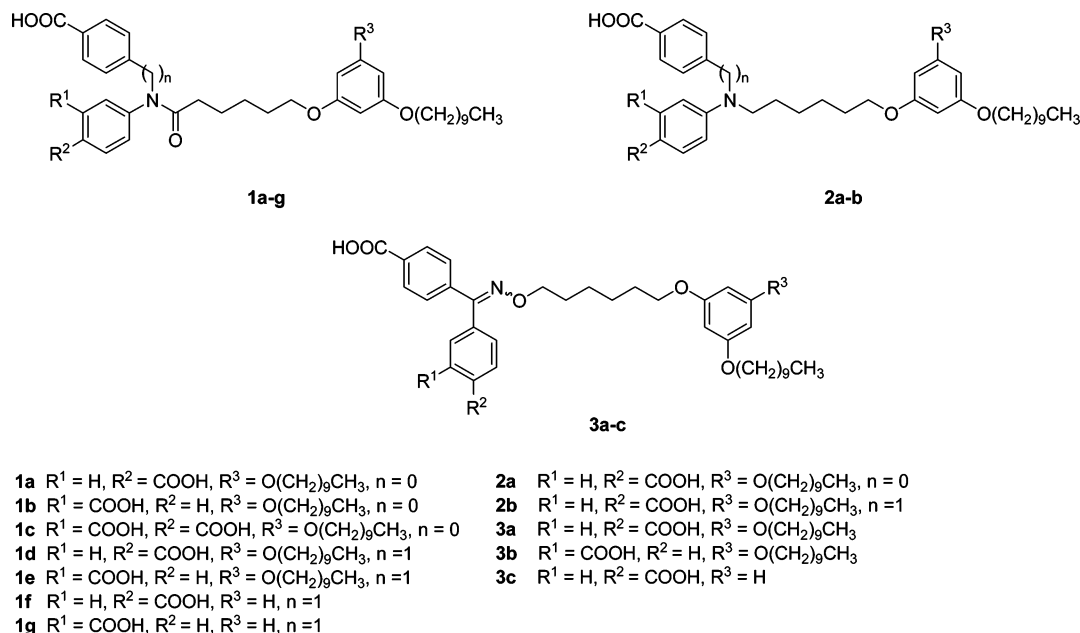


Figure 4. Synthetic targets.

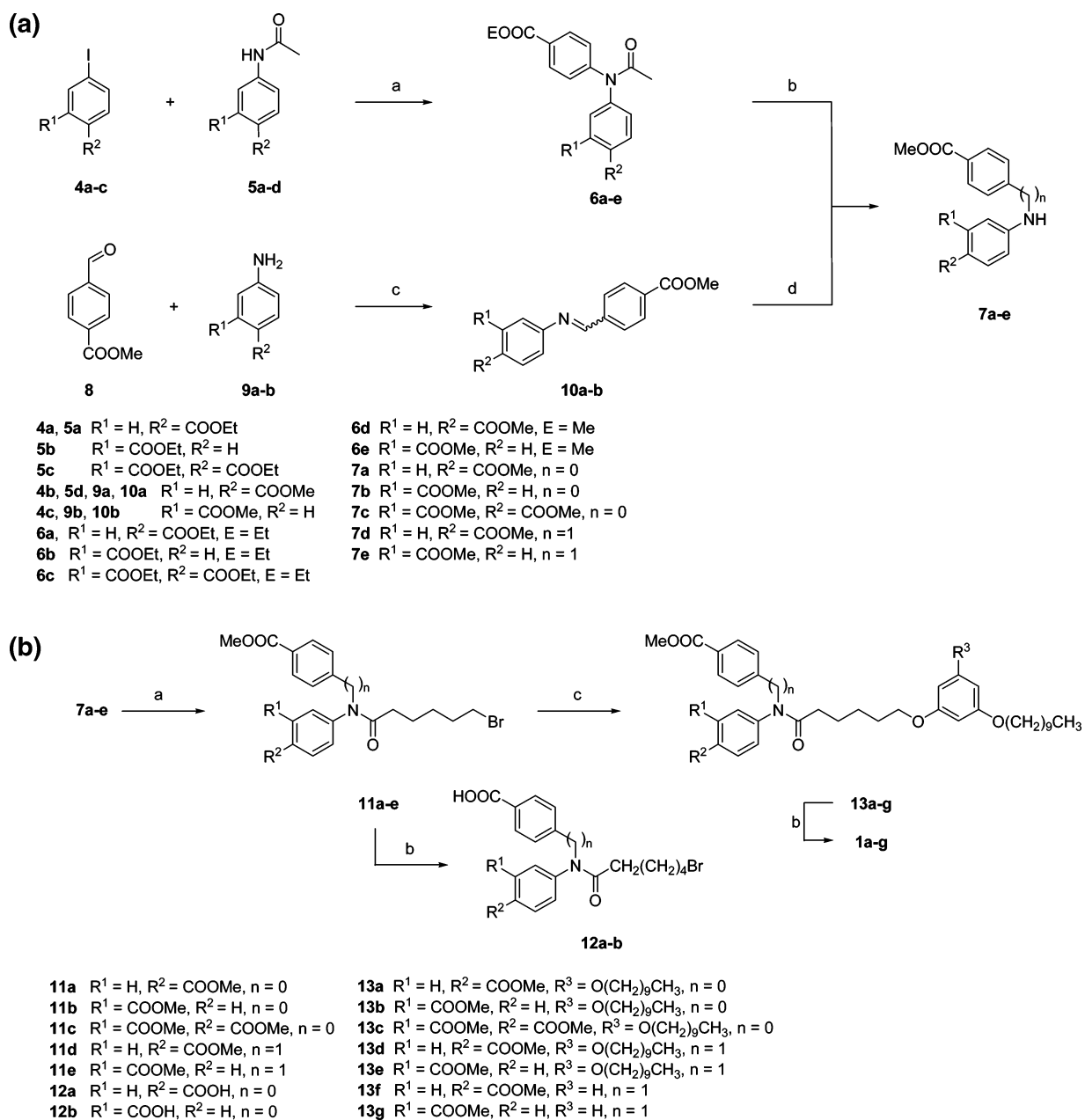
Coupling of **27** with **16** furnished the dichloro compound **28** in 80% yield in two steps.

Results and Discussion

As a primary screen for the antiadhesive activities of our synthesized compounds, we used a cell-based, computerized in vitro assay to quantify leukocyte adhesion to endothelial cells under static conditions.³⁷ In this assay compounds at 100 μ M were evaluated for inhibition of adhesion of MM6 cells to BAEC and sLe^x was chosen as reference. To compare the results for compounds that have been tested on different plates, the number of adherent MM6 cells on TNF- α -stimulated endothelial cells is set to 100% (Table 1). Advantages of this static cell-based assay are its reproducibility and the option for high-throughput screening. On the other hand, it has to be noted that rolling of leukocytes on activated endothelium mediated by selectin/oligosaccharide interactions is a nonequilibrium process that occurs under hydrodynamic flow. Therefore, static in vitro assays that measure inhibition under equilibrium conditions might generate data that are not predictive for in vivo activity of test compounds under flow conditions. To overcome this, potent compounds were further tested in our second assay. In a cell-based flow assay the ability of compounds to inhibit the adhesion of MM6 cells to recombinant selectin proteins was measured (see Experimental Section), whereas a cell-free, competitive ligand binding assay (glyco-ELISA) was applied to characterize selectin/ligand interactions.²⁹ The test principle in the cell-free assay involves immobilization of the used selectin onto an ELISA microtiter plate to which the substances and the ligand (sialyl Lewis^x tyrosinesulfate bound to biotinylated polyacrylamide) are added. After the incubation period the bound complex is detected by the streptavidin peroxidase reaction measuring the optical density at 414 nm in a microplate reader. The absorption of the empty plate is subtracted from all measured values. As control, we used wells only coated with sLe^x, whose values were set to 0%, and EDTA, which prevents the Ca²⁺-dependent selectin ligand binding completely (=100%). This demonstrates the specificity of the assay system. The results are indicated as proportional inhibition of the sLe^x binding. This assay takes full advantages of the fact that the interactions between the selectins and its carbohydrate ligands are low. The

consequence of the natural ligand binding weakly to the receptor necessitates the use of a multimeric presentation of the receptor or the ligand in the ELISA-based assays. For example, it is necessary to utilize streptavidin in this assay. A multimeric presentation ensures that a sufficient interaction survives wash steps and produces adequate signals to measure differences in inhibition of binding. For this reason this glyco-ELISA is more sensitive than comparable cell-free E-selectin binding assays. Furthermore, neutralizing anti-E-selectin antibodies completely blocked binding to E-selectin. This demonstrates the specificity of the assay system.³⁰ The compounds were simultaneously evaluated for their toxicity in the same cells using different assays (Table 2) to detect false positives.

Following the pharmacophore considerations by Kondo et al.¹⁸ (Figure 3a), three minimum criteria are supposed to be essential for activity: (I) a calcium ion binding structure, (II) a negatively charged group, and (III) a hydrophobic moiety. Therefore, several different groups were chosen as linker X to establish the carboxylic acid groups R¹–R² (Figure 3b) in the envisaged positions. Our original lead compound **1a** (Figure 1) proved to be potent in the static assay (100%) in our cell-based flow assay with an IC₅₀ of 35 \pm 26 μ M (n = 10) and showed inhibition of 58% in the P-selectin-ELISA assay at 500 μ M. But the major drawback of **1a** was a notable toxicity against MM6 cells (Table 2). We found that compounds containing a diphenylamide (**1a**) or -amino (**2a**), a phenylbenzylamide (**1f**) or -amino (**2b**), or a benzophenone oxime ether (**3a**) core structure, which act as spacers between the calcium binding substituent and the negatively charged residue at R¹–R², gave equivalent inhibitory activities in the static assay (100%, 107%, 93%, 100%, and 90%) (Table 1). A diphenylamide (**1a**), a phenylbenzylamide (**1e**), or amino scaffold (**2b**) as a bridge between the two carboxy groups led to analogues with potent adhesion blocking but significant cytotoxic profiles in the static assay. All tested methyl ester precursors, e.g., **21b** and **13a**, turned out to be less active or inactive in the static assay compared to the corresponding free acid derivatives **2b** and **1a** (61% and 10% vs 100% and 100%). The only exception was the phthalic acid dimethyl ester **13c**, which was as potent as its free acid derivative **1c** (115% vs 93%). Replacement of the carboxylic acid residues in **3a** by chloro atoms resulted in the

Scheme 1^a

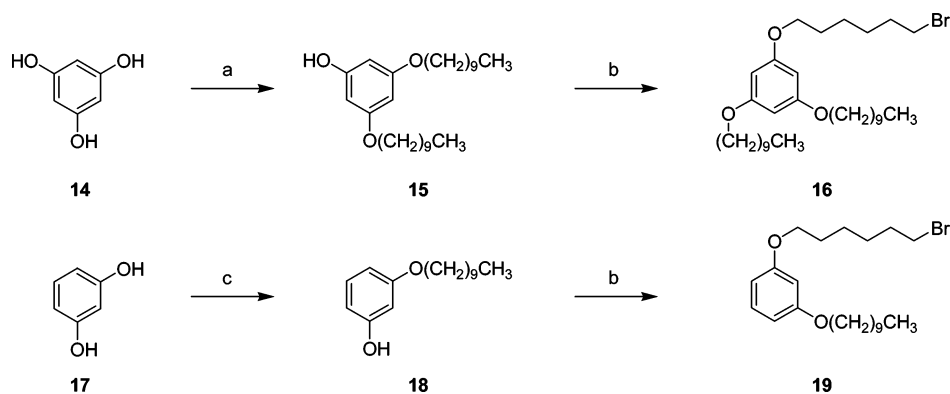
^a Reagents and conditions for part a: (a) method A (preparation of **7a-c**), Cu, CuI, K₂CO₃, *n*-Bu₂O, 4 days, reflux;¹⁹ method B (preparation of **7d,e**), CuI (1 mol %), K₃PO₄, *trans*-1,2-cyclohexanediamine (10 mol %), *n*-Bu₂O, 5 h, reflux; (b) NaOMe, MeOH, 1.5 h, reflux; (c) MeOH, 1 h, reflux; (d) NaBH₄, MeOH, 24 h, room temp. Reagents and conditions for part b: (a) NaH, *n*-Bu₂O, 2 h, room temp; 6-bromohexanoyl chloride, 4 h, reflux; (b) 0.5 M LiOH, THF, 8 h, 5 °C, then 16 h, 15 °C; (c) **15** or **18**, K₂CO₃, KI (or TBAD), cyclohexanone, 5 h, reflux.

quiet weak selectin blocker **28** (90% vs 24%), providing evidence that the presence of the carboxylic acid groups is essential for activity. In the course of our research we also investigated the influence of the carboxylic acid functions in different positions.

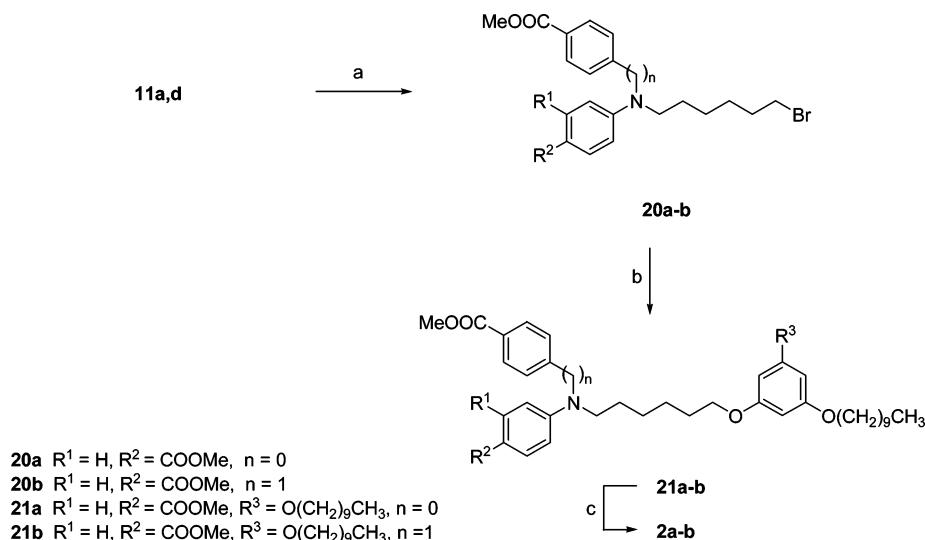
Our data suggest that in four of the most active selectin inhibiting compounds in the static assay (**1a**, 100%; **2b**, 100%; **13c**, 115%; **2a**, 107%) the carboxy group is located in the para position except for the phenylbenzylamide derivative **1e**, which carries one carboxylic acid in the meta position of the phenyl ring and possessed good inhibitory activity compared to its para, para substituted analogue **1d** (82% vs 56%).

To clarify the importance of the alkyl chains of the compounds toward the inhibitory activity, we have studied the active form of **2a**, like micellar species, in solution. Namely, we have measured the surface tension by the capillary rise method with

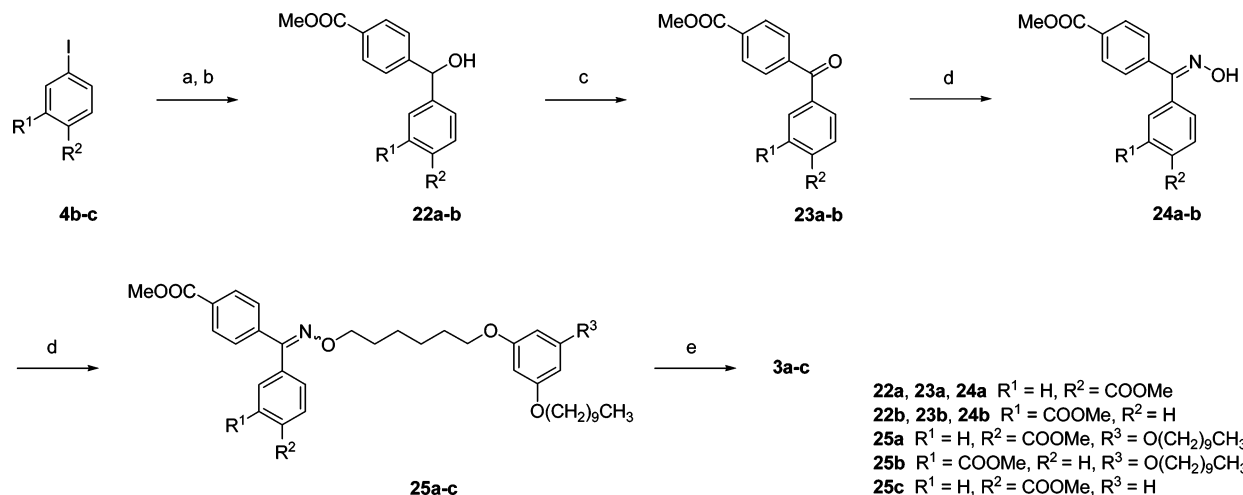
varying concentrations of compound **2a**.³⁰ As a result, the critical micelle concentration (cmc) could not be seen at IC₅₀ of 28 μM. These findings demonstrate that the alkyl chains with a moderate carbon length would be necessary for the strong bindings to all selectins. To verify to what extent the decyl chains are responsible for the selectin blocking activity or cytotoxicity, we were also seeking to replace the lipophilic side chains. When a phloroglucin ether group with two decyl chains (**3a**) was substituted for a resorcin ether group carrying only one decyl chain (**3c**), good activity was maintained in vitro (90% vs 67%) in the static cell based assay (Table 1). But the viability of MM6 cells was more potently diminished with **3c** as observed for **3a** (12% vs 84%). In contrast, the resorcin ether derivative **1f** combined potent selectin inhibitory activity (93%) with no loss in viability of BAEC (100%) whereas its phloroglucin analogue **1d** was less active (56%) by an augmented decrease

Scheme 2^a

^a Reagents and conditions: (a) 1-decanol, HCl-gas, 3 h, 70 °C; (b) 1,6-dibromohexane, K₂CO₃, cyclohexanone, reflux; (c) 1-bromodecane, EtOH, reflux, KOH.

Scheme 3^a

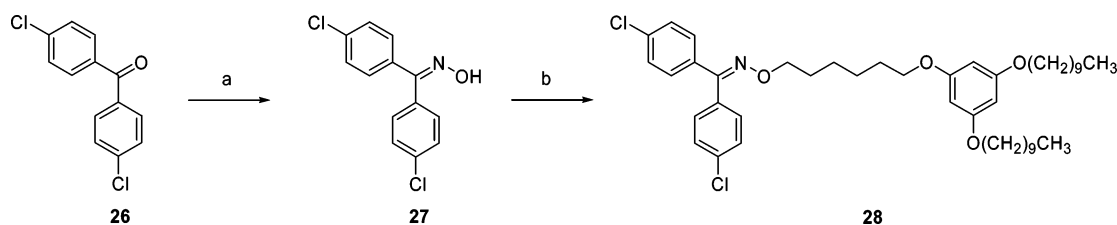
^a Reagents and conditions: (a) BH₃·THF, 1 h, reflux; (b) **15** or **18**, K₂CO₃, KI (or TBAI), cyclohexanone, 5 h, reflux; (c) 0.5 M KOH, THF, room temp.

Scheme 4^a

^a Reagents and conditions: (a) *i*-PrMgCl, THF, 40 min, -30 → -20 °C; (b) 4-formylbenzoic acid methyl ester **8**, THF, -20 °C, room temp, overnight; (c) PCC, CH₂Cl₂, 24 h, room temp; (d) HCl·H₂NOH, EtOH, NaOAc, 24 h, reflux; (e) **16** or **19**, NaH, DMF, TBAI, 2 h, room temp; (f) 0.5 M NaOH, EtOH/THF, 24 h, room temp.

in viability (36%). Taken together, no clear conclusion can be drawn in regard to the relationship of the activity, cytotoxicity, and the function of the decyl chains. For the purpose of determining the role of the hydrophobic tail in general, we also became interested in subjecting the synthetic precursors **12b**

and **12a**, in which the lipophilic didecyloxyphenoxy residue was not yet installed, to our test assays. As a result, the activity was completely lost when no hydrophobic tail was present (**12b** and **12a**, 2% vs 4%). To optimize the length of the side chains, groups with similar log *P* values will be evaluated in the future.

Scheme 5^a

^a Reagents and conditions: (a) HCl·H₂NOH, EtOH, NaOAc, 24 h, reflux; (b) **16**, NaH, DMF, TBAI, 2 h, room temp.

Table 1. In Vitro Potencies of the Compounds

compd	static assay ^a % inhibition at 100 μM	flow chamber assay ^{b,d} adherent MM6, E-selectin (100 μM) control (0%)	glyco-ELISA % inhibition E-selectin (100 μM) ^{c,d}	glyco-ELISA % inhibition P-selectin (500 μM) ^{c,d}	glyco-ELISA % inhibition L-selectin (500 μM) ^{c,d}
1a	100 ± 4	44 ± 3%, IC ₅₀ = 35 ± 20 μM	nt	58	53
1b	60 ± 9	50 ± 5%	nt	20	14
1c	93 ± 16	nt	62	102	102
1d	56 ± 12	nt	nt	49	50
1e	82 ± 19	nt	43 ± 5	95	92
1f	93 ± 18	nt	nt	nt	nt
1g	70 ± 11	nt	42	103	103
2a	107 ± 7	IC ₅₀ = 28 ± 7 μM	94	81 (35% at 100 μM)	82 (41% at 100 μM)
2b	100 ± 18	nt	nt	nt	nt
3a	90 ± 4	29 ± 10%, IC ₅₀ = 20 ± 14 μM	nt	2	6
3b	100 ± 15	68 ± 4%	nt	34	50
3c	67 ± 8	nt	nt	nt	nt
12a	4 ± 8	nt	5 ± 3	12	6
12b	2 ± 6	nt	nt	19	5
13a	10 ± 20	nt	5 ± 12 (500 μM)	16	16%
13c	115 ± 7	nt	73 (500 μM)	90	95
13d	26 ± 13	nt	nt	27	26
13f	26 ± 22	nt	65	78	75
13g	45 ± 16	nt	18	79	86
21b	61 ± 10	nt	nt	nt	nt
28	24 ± 8	nt	2	2	5
sLe ^x	41 ± 7	nt	nt	nt	nt

^a In this assay compounds at 100 μM were evaluated for inhibition of adhesion of MM6 cells to BAEC, and sLe^x was chosen as reference. To compare the results for compounds that have been tested on different plates, the number of adherent MM6 cells on TNF-α-stimulated endothelial cells is set to 100%. ^b In a cell-based flow assay the ability of compounds to inhibit the adhesion of MM6 cells to recombinant E-selectin protein was measured. Cells were counted as adhesive cells when they stuck at least 30 s to the plates. ^c The test principle in the cell-free assay involves immobilization of the used selectin onto an ELISA microtiter plate to which the substances and the ligand (sialyl Lewis^x tyrosinesulfate bound to biotinylated polyacrylamide) are added. After the incubation period the bound complex is detected by the streptavidin–peroxidase reaction, measuring the optical density at 414 nm in a microplate reader. The absorption of the empty plate is subtracted from all measured values. As control, we used wells only coated with sLe^x, whose values were set to 0%, and EDTA, which prevents the Ca²⁺-dependent selectin ligand binding completely (=100%). The results are indicated as proportional inhibition of the sLe^x binding. ^d nt = not tested.

Our findings are in line with previous conclusions by Slee et al.³¹ who investigated conceptually similar imidazole type compounds and observed that a hydrophobic side chain was required for potency in general. Slee also reported that the most potent derivatives in the cell-based assay systems contain a C16 alkyl chain and removal of the hydrophobic tail structure resulted in significant loss of activity. More recently, this was also supported by Girard et al.³² and Kaila et al.³³ who investigated quinic acid derivatives as sLe^x mimetics. All tested analogues missing such lipophilicity enhancing structural features have shown only moderate affinity. In both studies inhibitions ranged from 46% at 50 mM in a cell selectin assay³² to an IC₅₀ of 225 μM in a cell flow assay, and it could be demonstrated that presence of hydrophobic substituents resulted in a moderate increase in activity. By evaluation of the compounds in the glyco-ELISA, it was confirmed that inhibition of adhesion in the cell-based static assay was due to the inhibition of the specific ligand/receptor interactions. A good correlation was observed between the inhibition of adhesion in the static assay and the decrease in the binding of sLe^x toward E-, P-, and L-selectin. Among six compounds that showed inhibition of at least 80% in the cell adhesion assay, four compounds tested in the P- and L-selectin glyco-ELISA (**2a**, **1c**, **1e** and **13c**)

Table 2. In Vitro Cellular Toxicities of the Compounds

compd	% viability (XTT) ^{a,b} control (100%), MM6 (100 μM)	% viability (XTT) ^{a,b} control (100%), BAEC	% viability (ATP-lite) ^{a,b} control (100%)
1a	12 ± 2	107 ± 6	nt
1c	75 ± 7	nt	5
1d	nt	36 ± 7	nt
1e	11 ± 4	46 ± 7	0
1f	nt	100 ± 3	nt
1g	101 ± 5	20 ± 4	4
2a	112 ± 6	102 ± 10	77
2b	10 ± 2	nt	nt
3a	84 ± 2	110 ± 7	nt
3c	12 ± 1 (50 μM)	40 ± 1	nt
12b	nt	75 ± 5	nt
13c	50 ± 4	90 ± 7	58
13f	80 ± 4	nt	68
13g	98 ± 9	99 ± 10	62
21b	5 ± 1	111 ± 5	nt

^a To quantify antiproliferative and cytotoxic effects of our synthesized compounds, we employed the Roche-XTT assay and the ATP-lite assay. The assay is based on the conversion of the yellow tetrazolium salt XTT into an orange formazan dye by metabolically active cells. To compare the results for compounds that have been tested on different plates, the viability of untreated control cells is set to 100%. ^b nt = not tested.

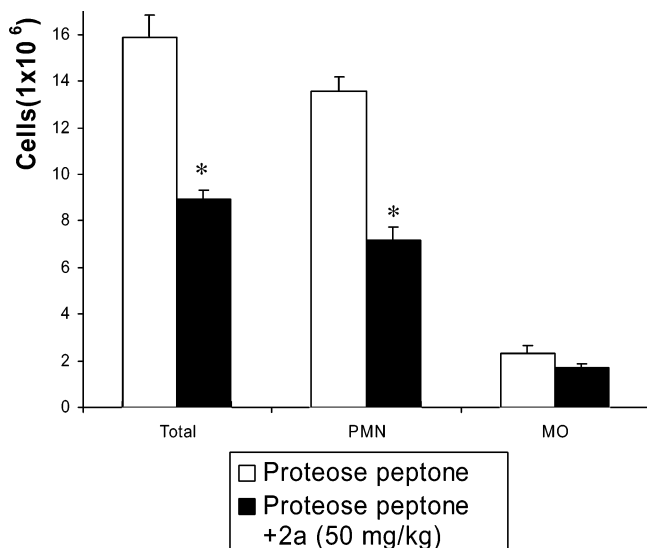


Figure 5. Effect of compound **2a** on leukocyte recruitment in proteose peptone induced mouse peritonitis. Leukocyte extravasation into the peritoneal cavity was analyzed in mice after intraperitoneal treatment with proteose peptone for 6 h (open bars). One group of animals received compound **2a** (50 mg/kg) intraperitoneally 1 h before challenge with proteose peptone (black bars). Leukocytes harvested from the peritoneal cavity after 6 h were stained with subgroup specific PE-conjugated antibodies and differentiated according to forward and side scatter parameters and fluorescence intensity. Values are the mean \pm SEM of four independent experiments: (*) $P < 0.05$ vs control.

possessed a selectin-inhibiting potency in the same manner. Surprisingly, **1a** showed a weak potency and **3a** failed to reduce binding of sLe^x toward P- and L-selectin (58% vs 53% and 2% vs 6%) despite excellent activity in our static assay (100% vs 90%). From analysis of the reverse case, with substances that cause a small or a not notable inhibition of adhesion in the static assay, the corresponding results in the glyco-ELISA assay could be observed (**13a**, **12b**, **12a**, **13d**, and **1d**); i.e., no compound with less activity in the cell-based static assay was potent in the selectin binding assay.

There were four compounds (**2a**, **1c**, **13c**, **1e**) that showed high potency in the cell-based static assay and the P- and L-selectin glyco-ELISA binding assays, but only **2a** had a favorable toxicity profile in all cytotoxicity assays. Thus, compound **2a** was further evaluated in the E-selectin cell flow chamber assay where it proved to inhibit rolling and adhesion with an IC₅₀ of $28 \pm 7 \mu\text{M}$ (Table 1). In addition, **2a** turned out to be nontoxic in an additional ATP-lite toxicity assay, a standard method used to monitor cell proliferation. Consequently, **2a** was chosen for further in vivo evaluation. The effect of **2a** on leukocyte recruitment in vivo was tested in a mouse peritonitis model. Leukocyte extravasation was induced by ip proteose peptone (3%) treatment. As seen in Figure 5, pretreatment with **2a** (50 mg/kg) reduced the total cell count in the peritoneal cavity, the majority of which were PMNs (−44%) ($n = 4$, $P < 0.05$).³⁴ Only few monocytes and lymphocytes were extravasated in response to proteose peptone stimulation. sLe^x was inactive in this model of acute inflammation at doses up to 100 mg/kg.³⁵ This indicates that our in vitro selectin assays predicted anti-inflammatory efficacy of the test compound in vivo.

Our proposed model of the binding mode calculated by the software for the diphenylamino-based inhibitor **2a** to E-selectin is illustrated in Figure 6. It shows that compounds with a diphenylamino structure can likewise bind to E-selectin according to the forecasts of the pharmacophore model. A carboxylic

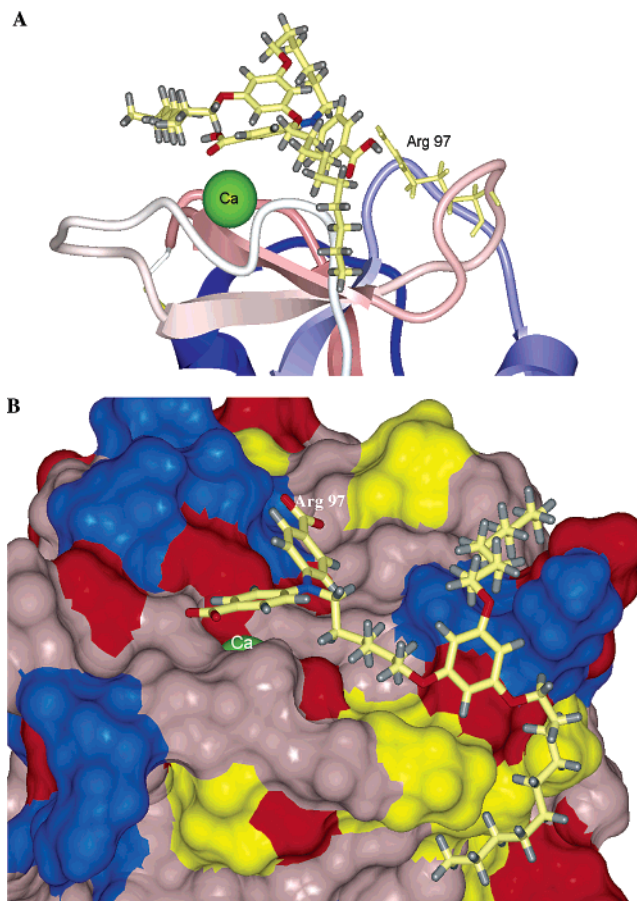


Figure 6. (A) Docking model of a ribbon representation of **2a** bound to E-selectin (PDB-code: 1G1T). The E-selectin calcium is shown as a green sphere. (B) Compound **2a** docked into the binding site of E-selectin. The accessible surface of the binding site of E-selectin was calculated with ICM-Pro and is colored by lipophilicity: Hydrophobic amino acids are yellow (Ala, Val, Phe, Met, Ile, Leu), hydrophilic amino acids are gray (Ser, Thr, Tyr, His, Cys, Asn, Gln, Trp, Gly), positive charged amino acids are blue (Lys, Arg), and negative charged amino acids are red (Asp, Glu).

acid group orients itself to the Ca²⁺ ion, filling out the coordination sphere in a manner similar to the way the fucose subunit is believed to bind in the natural ligand structure sLe^x. The second carboxy group is directed to Arg97 (E-selectin) or to Lys99 in the case of P-selectin, while the alkyl chains interact almost completely in hydrophobic regions of the E-selectin surface (Figure 6B; yellow amino acids are Ala, Val, Phe, Met, Ile, Leu). This binding mode demonstrates that the molecule part between the polar headgroup and the hydrophobic tail, the so-called “spacer” group, fulfills its purpose. This group is arranged in a way that it sticks out from the binding pocket of the polar groups, and so it keeps the hydrophobic molecule part from this region away. Thereby the alkyl chains can bind themselves within somewhat more distant hydrophobic areas of the E-selectin surface.

Overall, when we compare the proposed binding mode of our inhibitors to that of the known natural ligand sLe^x (Figure 1), we suppose that the two carboxylic acids act as replacements for the critical fucose and sialic acid subunits of sLe^x, with a diarylamino scaffold replacing the lactosamine structure. This proposed binding mode is similar to that discussed by Kogan et al.³⁶ for the mannose-containing inhibitor bimosiamose. If the mode of binding is indeed similar, our series of compounds suggest that the proposed calcium binding mannose residue of bimosiamose can be replaced by a simple carboxylic acid,

resulting in a completely novel sLe^x mimetic containing no more carbohydrates.

Summary

Novel and potent small-molecule pan-selectin inhibitors have been developed. A combination of synthesis and structure-based design allowed rapid optimization, resulting in compounds with in vivo activity. We exploited the three minimal criteria that are essential for activity: (1) a calcium ion binding moiety, (2) a negatively charged group, and (3) a hydrophobic tail structure (Figure 3). Of those that were tested, the presence of two carboxylic acids was found to be optimal. One carboxylic acid of a benzoic acid derivative coordinates to calcium and the other undergoes electrostatic interactions with Arg97 (E-selectin) and/or Lys99 (P-selectin). As several different spacers were tolerated, we believe that a number of templates can be used to combine the carboxylic acid groups.

Taken together, the ligand binding glyco-ELISA assays, the cell-selectin flow chamber assay, and the static cell–cell assay systems proved to be essential for lead optimization and seemed to give more predictive results in terms of identifying compounds with in vivo activity. Several members of this series were found to be active E-, P-, and L-selectin inhibitors. One of the more potent derivatives, compound **2a**, identified as having good activity and negligible toxicity in vitro, was shown to reduce inflammation in vivo. This novel class of nonglycosidic and nonpeptidic pan-selectin blockers opens up new possibilities for the development of therapeutic agents in inflammatory disease. In the course of our ongoing research project, further investigations are currently undertaken.

Experimental Section

Static Assay. The adhesion assay was performed as described previously.³⁷ Briefly, BAEC monolayers 7 days after seeding, passage 1–3, were grown in 24-well plates. Prior to assay, the BAEC samples were examined microscopically to confirm the integrity and uniformity of the monolayers. After the culture medium was removed and the endothelial cell monolayer was washed with DPBS (2 × 1 mL/well at 37 °C), the cells were treated with cell culture medium containing 20 ng/mL recombinant tumor necrosis factor α (TNFα) for 4 or 16 h and the respective test substance was dissolved in DMSO or vehicle for 20 min (in other settings for 4 or 16 h) at 37 °C/5% CO₂. The BAEC samples were washed with DPBS (2 × 1 mL/well at 37 °C) before 900 μL of culture medium and 100 μL of PMN suspension (1 × 10⁶ cells/mL) per well were added and incubated for 30 min at 37 °C/5% CO₂. Nonadherent PMNs were removed by washing with DPBS (3 × 1 mL/well at 37 °C). Culture medium (1 mL/well at 37 °C) was added prior to microscopic examination. (In inhibition experiments, various concentrations of drugs were used (1 × 10⁻⁴ to 1 × 10⁻⁷ mol/L).) After incubation with cytokines or drugs, the cell viability of BAEC was confirmed by trypan blue exclusion and additional microscopic examination. IC₅₀ values were calculated using the program GRAFIT, Erithacus Software Ltd., U.K.

E-Selectin-Cell Adhesion Assays. The ability of compounds to inhibit the adhesion of MM6 cells to pure selectin proteins was measured using a “cell-selectin” assay. Recombinant soluble E-selectin protein purchased from R&D Systems (Minneapolis, MN) was diluted to 5 μg/mL in Dulbecco’s PBS containing calcium and magnesium ions (PBS+). Plates coated with recombinant E-selectin were produced by adding 50 μL of the protein (5 μg/mL) to the center of a well in a six-well plate and stored overnight at 4 °C. The selectin protein was omitted from negative control (“background”) wells. The plates were washed with 3 × 100 μL of PBS+ and incubated for 60 min with 100 μL of a solution of the test compounds (or vehicle controls) in RPMI (containing 1% FCS and DMSO) in the final test concentration. After the plates

were washed with 3 × 100 μL of PBS+, a flat-polished flow chamber (Glycotech) was placed on the surface of the well and MM6 or PMNs, suspended at 1 × 10⁶ cells/mL in RPMI medium plus 1% FCS, were perfused through the flow chamber at a constant shear stress of 1 dyn/cm² for 4 min. Rolling and adherent leukocytes were visualized and counted in each well in four separate randomly chosen fields within the first minute, applying an inverted phase contrast microscope connected to a video camera (Kappa CF 15/2) and a video recorder (Panasonic SVHS TL700). All experiments were repeated two or three times. IC₅₀ values were calculated with the program GRAFIT, Erithacus Software Ltd., U.K.

Protease Peptone Induced Mouse Peritonitis. Male C57BL/6 mice were subjected to intraperitoneal injection of 3 mL of 3% protease peptone (Oxoid Ltd.) 1 h after ip treatment with 100 μL of a suspension of test compound (50 mg/mL) in corn oil. Vehicle only was used as control. Protease peptone is a breakdown product of proteins that has been widely shown to possess strong capacity to stimulate leukocyte recruitment to extravascular tissue. After 6 h, leukocytes were harvested from the peritoneum with 3 mL of cold HBSS containing 5 mM EDTA. Samples were centrifuged (2000 rpm for 5 min), labeled with 5 μL of PE conjugated rat antimouse macrophage/monocyte antibody (MOMA-2, ImmunoKontakt), antimouse PMN antibody (anti-PMN, ImmunoKontakt), and antimouse T-lymphocyte antibody (anti-CD2, ImmunoKontakt) for 20 min at 4 °C, washed twice, and resuspended in HBSS. Gating for leukocyte subpopulations was based on forward and side scatter parameters and FL-1.

Description of Docking Programs and Settings. Molecular models of candidate molecules were generated by using the ab initio, flexible docking procedure of the ICM (version 3.0) molecular modeling program by Molsoft. Structural coordinates for the “receptor” were derived from the cocrystal structure of sLe^x bound to the E-selectin from which the ligand was removed. Receptor grid maps were calculated with a grid spacing of 0.5 Å. The grid was defined in such a way that it included the ligand and key residues plus 3–5 Å in each of the x, y, z directions. For the ligands, 2D to 3D conversion is followed by energy minimization using the MMFF option as a force field. The docking algorithm implemented in ICM (version 3.0) optimizes the entire ligand in the receptor field, applying a multistart Monte Carlo minimization procedure in internal coordinate space. The Metropolis temperature for accepting or rejecting a new pose was set to 600 K. The number of Monte Carlo steps and iterations of the local energy minimization was determined automatically by an adaptive algorithm depending on the size and number of flexible torsions in the ligand. More details can be found in refs 38 and 39.

6-Bromohexanoic Acid *N,N*-Bis(4-carboxyphenyl)amide (12a). A solution of **11a** (150 mg, 0.324 mmol) in THF (8 mL) was stirred with an aqueous lithium hydroxide solution (0.5 M, 1.95 mL, 0.97 mmol) solution at 5 °C for 8 h and at 15 °C for another 16 h. Subsequently, water (20 mL) was added and the mixture was extracted with ether twice. The organic extracts were discarded, and the aqueous layer was acidified to pH 1 by dropwise addition of aqueous hydrochloric acid (1.0 M) and extracted with ether (3 × 8 mL). The combined organic layers were washed with water and brine, dried over MgSO₄, and concentrated. The crude product was recrystallized from methanol to yield 114 mg (81%) of **12a** as a colorless solid. Mp 150–151 °C; ¹H NMR (DMSO-*d*₆) δ 13.09 (s_{br}, 2H), 7.97 (d, 8.1 Hz, 4H), 7.45 (d, 8.1 Hz, 4H), 3.49 (t, 6.6 Hz, 2H), 2.24 (t, 7.4 Hz, 2H), 1.78–1.65 (m, 2H), 1.65–1.50 (m, 2H), 1.39–1.27 (m, 2H); MS (FD) *m/z* 435 (M⁺ for Br⁸¹) and 433 (M⁺ for Br⁷⁹). Anal. (C₂₀H₂₀BrNO₅) C, H, N.

6-Bromohexanoic Acid *N,N*-3,4'-Bis(carboxyphenyl)amide (12b). Dimethyl ester **11b** (250 mg, 0.541 mmol) in THF (13 mL) was stirred with an aqueous lithium hydroxide solution (0.5 M, 3.06 mL, 1.53 mmol), employing the procedure for the preparation of dicarboxylic acid **12a** to give 201 mg (86%) of **12b** as a colorless solid. Mp 190–191 °C; ¹H NMR (DMSO-*d*₆) δ 11.71 (s_{br}, 2H), 7.96 (d, 8.4 Hz, 2H), 7.87 (d, 7.2 Hz, 1H), 7.84 (s, 1H), 7.70–7.41 (m, 4H), 3.48 (t, 6.7 Hz, 2H), 2.22 (t, 7.4 Hz, 2H), 1.78–1.65 (m,

2H), 1.65–1.50 (m, 2H), 1.39–1.27 (m, 2H); MS (FD) m/z 435 (M^+ for Br^{81}) and 433 (M^+ for Br^{79}). Anal. ($C_{20}H_{20}BrNO_5$) C, H, N.

6-(3,5-Didecyloxyphenoxy)hexanoic Acid *N,N*-Bis(4-carboxyphenyl)amide (1a). **13a** (500 mg, 0.635 mmol) was dissolved in THF (16 mL) and stirred with an aqueous lithium hydroxide solution (0.5 M, 3.81 mL, 1.90 mmol) at 5 °C for 8 h and at 15 °C for another 16 h. Subsequently, water (50 mL) was added and the mixture was extracted with ether once. A suitable separation of the layers was achieved by storing the emulsion in a refrigerator at 5 °C overnight. The ethereal extract was separated and discarded. The remaining aqueous layer was acidified to pH 1 by the dropwise addition of aqueous hydrochloric acid (1.0 M solution) and extracted with ether. The combined organic layers were washed with water and brine, dried over $MgSO_4$, and concentrated. The crude product was recrystallized from methanol to yield 428 mg (89%) of **1a** as a colorless solid. Mp 158–160 °C; IR (KBr) 3030, 2890, 2820, 2640, 2520, 1660, 1580 cm^{-1} ; 1H NMR ($CDCl_3$) δ 8.13 (d, 8.6 Hz, 4H), 7.33 (d, 8.6 Hz, 4H), 6.06 (t, 2.1 Hz, 1H), 6.03 (d, 2.1 Hz, 2H), 3.88 (d, 6.4 Hz, 6H), 2.33 (t, 7.2 Hz, 2H), 1.81–1.67 (m, 8H), 1.51–1.21 (m, 30H), 0.87 (t, 6.7 Hz, 6H); MS (FD) m/z 760 (M^+). Anal. ($C_{46}H_{65}NO_8$) C, H, N.

6-(3,5-Didecyloxyphenoxy)hexanoic Acid *N,N*-3,4'-Bis(carboxyphenyl)amide (1b). Dimethyl ester **13b** (463 mg, 0.588 mmol) in THF (15 mL) was stirred with an aqueous lithium hydroxide solution (0.5 M, 3.53 mL, 1.76 mmol) using the procedure described for the preparation of dicarboxylic acid **1a** to give 300 mg (67%) of **1b** as a colorless solid. 1H NMR ($DMSO-d_6$, 500 MHz, 323 K) δ 7.95 (d, 8.6 Hz, 2H), 7.87 (d, 7.8 Hz, 1H), 7.83 (t, 2.0 Hz, 1H), 7.60 (d, 7.8 Hz, 1H), 7.53 (t, 7.8 Hz, 1H), 7.43 (d, 8.6 Hz, 2H), 6.01 (s, 3H), 3.90–3.83 (m, 6H), 2.24 (t, 7.4 Hz, 2H), 1.69–1.55 (m, 8H), 1.41–1.19 (m, 30H), 0.84 (t, 6.9 Hz, 6H); MS (FD) m/z 760 (M^+). Anal. ($C_{46}H_{65}NO_8$) C, H, N.

6-(3,5-Didecyloxyphenoxy)hexanoic Acid *N*-(4-Carboxyphenyl)-*N*-(3,4-dicarboxyphenyl)amide (1c). A solution of the trimethyl ester **13c** (239 mg, 0.28 mmol) in THF (11 mL) was treated with an aqueous solution of lithium hydroxide (0.5 M, 2.26 mL, 1.13 mmol) according to the procedure described for the preparation of compound **1a** so that an amount of 161 mg (71%) of **1c** was isolated as a colorless resin. 1H NMR ($CDCl_3$) δ 8.07 (d, 8.1 Hz, 2H), 7.81 (d, 8.1 Hz, 1H), 7.57–7.47 (m, 2H), 7.30 (d, 8.1 Hz, 2H), 6.05 (t, 1.9 Hz, 1H), 6.02 (d, 1.9 Hz, 2H), 3.94–3.81 (m, 6H), 2.38–2.24 (m, 2H), 1.82–1.64 (m, 8H), 1.47–1.18 (m, 30H), 0.86 (t, 6.7 Hz, 6H); MS (FD) m/z 805 ($M^+ + 1$). Anal. ($C_{47}H_{65}NO_{10}$) C, H, N.

6-(3,5-Didecyloxyphenoxy)hexanoic Acid *N*-(4-Carboxybenzyl)-*N*-(4-carboxyphenyl)amide (1d). Dimethyl ester **13d** (443 mg, 0.552 mmol) dissolved in THF (14 mL) was stirred with an aqueous solution of lithium hydroxide (0.5 M, 3.31 mL, 1.66 mmol) using the procedure for the preparation of **1a**. Thus, an amount of 343 mg (80%) of the desired dicarboxylic acid **1d** was obtained as a colorless resin. 1H NMR ($CDCl_3$) δ 8.08 (d, 8.6 Hz, 2H), 8.01 (d, 8.4 Hz, 2H), 7.29 (d, 8.4 Hz, 2H), 7.10 (d, 8.6 Hz, 2H), 6.05 (t, 1.9 Hz, 1H), 6.02 (d, 1.9 Hz, 2H), 5.01 (s, 2H), 3.92–3.83 (m, 6H), 2.16 (t, 7.4 Hz, 2H), 1.80–1.62 (m, 8H), 1.49–1.21 (m, 30H), 0.87 (t, 6.7 Hz, 6H); MS (FD) m/z (%) 774 (M^+). Anal. ($C_{47}H_{67}NO_8$) C, H, N.

6-(3,5-Didecyloxyphenoxy)hexanoic Acid *N*-(4-Carboxybenzyl)-*N*-(3-carboxyphenyl)amide (1e). A solution of the dimethyl ester **13e** (425 mg, 0.530 mmol) in THF (13 mL) was treated with an aqueous lithium hydroxide solution (0.5 M, 3.18 mL, 1.59 mmol), employing the procedure given for the preparation of compound **1a** to provide 312 mg (76%) of **1e** as a colorless resin. 1H NMR ($CDCl_3$) δ 8.05 (d, 7.9 Hz, 1H), 8.01 (d, 8.1 Hz, 2H), 7.62 (s, 1H), 7.48 (t, 7.9 Hz, 1H), 7.33–7.25 (m, 3H), 6.04 (t, 1.9 Hz, 1H), 6.01 (d, 1.9 Hz, 2H), 4.99 (s, 2H), 3.91–3.81 (m, 6H), 2.12 (t, 7.4 Hz, 2H), 1.79–1.62 (m, 8H), 1.46–1.17 (m, 30H), 0.87 (t, 6.7 Hz, 6H); MS (FD) m/z 774 (M^+). Anal. ($C_{47}H_{67}NO_8$) C, H, N.

6-(3-Decyloxyphenoxy)hexanoic Acid *N*-(4-Carboxybenzyl)-*N*-(4-carboxyphenyl)amide (1f). A solution of dimethyl ester **13f**

(471 mg, 0.73 mmol) in THF (18 mL) was treated with an aqueous solution of lithium hydroxide (0.5 M, 4.38 mL, 2.19 mmol), applying the procedure reported for the preparation of dicarboxylic acid **1a** to achieve 339 mg (75%) of **1f** as a colorless solid. Mp 167–168 °C; 1H NMR ($CDCl_3$) δ 8.08 (d, 8.6 Hz, 2H), 8.01 (d, 8.4 Hz, 2H), 7.29 (d, 8.4 Hz, 2H), 7.13 (t, 7.9 Hz, 1H), 7.10 (d, 8.4 Hz, 2H), 6.50–6.40 (m, 3H), 5.01 (s, 2H), 3.94–3.85 (m, 4H), 2.17 (t, 7.4 Hz, 2H), 1.81–1.64 (m, 6H), 1.47–1.20 (m, 16H), 0.87 (t, 6.7 Hz, 2H); MS (FD) m/z 618 (M^+). Anal. ($C_{37}H_{47}NO_7$) C, H, N.

6-(3-Decyloxyphenoxy)hexanoic Acid *N*-(4-Carboxybenzyl)-*N*-(3-carboxyphenyl)amide (1g). Dimethyl ester **13g** (336 mg, 0.520 mmol) was dissolved in THF (13 mL) and stirred with an aqueous lithium hydroxide solution (0.5 M, 3.12 mL, 1.56 mmol) following the procedure for the preparation of dicarboxylic acid **1a** so that an amount of 258 mg (80%) of **1g** was obtained as a colorless solid. Mp 134–135 °C; 1H NMR ($CDCl_3$) δ 8.06 (d, 8.1 Hz, 1H), 8.01 (d, 8.1 Hz, 2H), 7.67 (s, 1H), 7.47 (t, 7.9 Hz, 1H), 7.32–7.26 overlapping signals (7.29, d, 8.4 Hz, 2H and m, 1H), 7.12 (t, 8.1 Hz, 1H), 6.49–6.39 (m, 3H), 4.99 (s, 2H), 3.94–3.84 (m, 4H), 2.13 (t, 7.4 Hz, 2H), 1.81–1.63 (m, 6H), 1.49–1.21 (m, 16H), 0.87 (t, 6.7 Hz, 3H); MS (FD) m/z 618 (M^+). Anal. ($C_{37}H_{47}NO_7$) C, H, N.

4-[*N*-(6-(3,5-Bis(decyloxy)phenoxy)hexyl)-*N*-(4-(carboxyphenyl)amino)benzoic Acid (2a). A solution of dimethyl ester **21a** (123 mg, 0.160 mmol) in THF (5 mL) was stirred with an aqueous potassium hydroxide solution (0.5 M, 0.96 mL, 0.480 mmol) at room temperature according to the procedure for the preparation of **1a** to give 86 mg (73%) of **2a** as a colorless solid. 1H NMR ($CDCl_3$) δ 8.03 (d, 8.8 Hz, 4H), 7.10 (d, 8.8 Hz, 4H), 6.09–6.03 (m, 3H), 3.94–3.78 overlapping signals (3.89, t, 6.4 Hz, 6H and m, 2H), 1.81–1.67 (m, 8H), 1.54–1.19 (m, 32H), 0.88 (t, 6.7 Hz, 6H); MS (FD) m/z 746 (M^+). Anal. ($C_{46}H_{67}NO_7$) C, H, N.

4-[*N*-(4-Carboxybenzyl)-*N*-(6-bis(3,5-decyloxyphenoxy)hexylamino)benzoic Acid (2b). Dimethyl ester **21b** (301 mg, 0.38 mmol) was dissolved in THF (5 mL) and treated with an aqueous potassium hydroxide solution (0.5 M, 2.28 mL, 1.14 mmol) at room temperature following the procedure for the preparation of **1a** to give 196 mg (68%) of **2b** as a colorless resin. 1H NMR ($CDCl_3$) δ 7.99 (d, 8.3 Hz, 2H), 7.85 (d, 9.0 Hz, 2H), 7.21 (d, 8.3 Hz, 2H), 6.55 (d, 9.1 Hz, 2H), 5.99–5.90 (m, 3H), 4.61 (s, 2H), 3.86–3.79 (m, 6H), 3.44 (t, 6.9 Hz, 2H), 1.73–1.62 (m, 6H), 1.40–1.30 (m, 2H), 1.19–0.97 (m, 32H), 0.80 (t, 6.9 Hz, 6H); MS (EI) m/z 761 ($M^+ + 1$). Anal. ($C_{47}H_{69}NO_7$) C, H, N.

O-[6-(3,5-Didecyloxyphenoxy)hexyl]-4,4'-bis(carboxyphenyl)methanone Oxime (3a). **25a** (500 mg, 0.623 mmol) was dissolved in a mixture of ethanol (5.10 mL) and THF (12.3 mL) and stirred with an aqueous sodium hydroxide solution (0.5 M, 3.75 mL) at room temperature for 24 h. Subsequently, water (30 mL) was added and the mixture was extracted with Et_2O once. The ether extract was discarded. The aqueous layer was acidified to pH 6–5 by the dropwise addition of 1 M aqueous hydrochloric acid and extracted with ether. The combined ethereal extracts were washed with water and brine and dried over Na_2SO_4 to provide 458 mg (95%) of **3a** as a colorless resin. 1H NMR ($CDCl_3$) δ 8.21 (d, 8.4 Hz, 2H), 8.09 (d, 8.4 Hz, 2H), 7.58 (d, 8.4 Hz, 2H), 7.45 (d, 8.4 Hz, 2H), 6.05 (s, 3H), 4.24 (t, 6.4 Hz, 2H), 3.89 (t, 6.4 Hz, 6H), 1.81–1.68 (m, 8H), 1.51–1.22 (m, 32H), 0.87 (t, 6.7 Hz, 6H); MS (FD) m/z 774 (M^+). Anal. ($C_{47}H_{67}NO_8$) C, H, N.

O-[6-(3,5-Didecyloxyphenoxy)hexyl]-3,4'-bis(carboxyphenyl)methanone Oxime (3b). Following the procedure for the preparation of compound **3a**, a solution of dimethyl ester **25b** (341 mg, 0.425 mmol) in THF (8.5 mL) and ethanol (3.5 mL) was stirred with an aqueous sodium hydroxide solution (0.5 M, 2.55 mL, 1.28 mmol) to give 287 mg (87%) of **3b** as a colorless resin. 1H NMR ($CDCl_3$) δ 8.22–8.03 (m, 4H), 7.64–7.42 (m, 4H), 6.05 (s, 3H), 4.24 (t, 6.4 Hz, 2H), 3.89 (t, 6.4 Hz, 6H), 1.81–1.67 (m, 8H), 1.54–1.21 (m, 32H), 0.87 (t, 6.7 Hz, 6H); MS (FD) m/z 774 (M^+). Anal. ($C_{47}H_{67}NO_8$) C, H, N.

O-[6-(3-Decyloxyphenoxy)hexyl]-4,4'-bis(carboxyphenyl)methanone Oxime (3c). A solution of the dimethyl ester **25c** (357

mg, 0.553 mmol) in a mixture of THF (11 mL) and ethanol (4.5 mL) was treated with an aqueous sodium hydroxide solution (0.5 M, 3.65 mL, 1.82 mmol) using the procedure reported for the preparation of the dicarboxylic acid **3a** to provide 321 mg (94%) of **3c** as a colorless resin. ¹H NMR (CDCl₃) δ 8.20 (d, 8.4 Hz, 2H), 8.08 (d, 8.6 Hz, 2H), 7.58 (d, 8.6 Hz, 2H), 7.45 (d, 8.4 Hz, 2H), 7.15 (t, 8.1 Hz, 1H), 6.51–6.43 (m, 3H), 4.25 (t, 6.7 Hz, 2H), 3.92 (t, 6.4 Hz, 4H), 1.83–1.69 (m, 6H), 1.55–1.20 (m, 18H), 0.87 (t, 6.7 Hz, 3H); MS (FD) *m/z* 618 (M⁺). Anal. (C₃₇H₄₇NO₇) C, H, N.

O-[-6-(3,5-Didecyloxyphenoxy)hexyl]bis(4-chlorophenyl)-methanone Oxime (28). A solution of **27** (234 mg, 0.878 mmol) in dry DMF (3 mL) was treated with sodium hydride (60% in mineral oil, 40.4 mg, 1.01 mmol) and subsequently reacted with **16** (500 mg, 0.878 mmol) in the presence of a catalytic amount of *n*-Bu₄NI according to the procedure described for the preparation of compound **25a**. After column chromatography (silica gel, ethyl acetate/petroleum ether 1:15), an amount of 581 mg (88%) of **28** was obtained as a colorless oil. ¹H NMR (CDCl₃) δ 7.40 (d, 8.6 Hz, 4H), 7.32–7.24 (m, 4H), 6.07–6.03 (m, 3H), 4.18 (t, 6.7 Hz, 2H), 3.89 (t, 6.7 Hz, 6H), 1.81–1.66 (m, 8H), 1.52–1.21 (m, 32H), 0.88 (t, 6.7 Hz, 6H); MS (FD) *m/z* (%) 758 (M⁺ + 3, 27), 757 (M⁺ + 2, 60), 756 (M⁺ + 1, 41), 755 (M⁺, 100). Anal. (C₄₅H₆₅-Cl₂NO₄) C, H, N.

Acknowledgment. This study was supported by grants from the Deutsche Pharmazeutische Gesellschaft and Fonds der Chemischen Industrie, the Swedish Research Council, the Swedish Heart-Lung Foundation, and the AFA Health Fund. H.K.U. and O.S. thank the Deutsche Forschungsgemeinschaft (Grant UL-199/1-2 and SO 876/1-1) for financial support. We thank the Revotar AG for their collaboration. Their work was supported by grants of the Ministry of Economics of the State of Brandenburg and the European Union. The authors thank Prof. Dr. Pindur for the opportunity to perform the ICM (version 3.0) investigations.

Supporting Information Available: Additional experimental procedures, characterization of new compounds, and references to known procedures. This material is available free of charge via the Internet at <http://pubs.acs.org>.

References

- Ulbrich, H.; Eriksson, E. E.; Lindbom, L. Leukocyte and endothelial cell adhesion molecules as targets for therapeutic interventions in inflammatory disease. *Trends Pharmacol. Sci.* **2003**, *24*, 640–647.
- Ehrhardt, C.; Kneuer, C.; Bakowsky, U. Selectins, an emerging target for drug delivery. *Adv. Drug Delivery Rev.* **2004**, *56*, 527–549.
- Szekanecz, Z.; Koch, A. E. Therapeutic inhibition of leukocyte recruitment in inflammatory diseases. *Curr. Opin. Pharmacol.* **2004**, *4*, 423–428.
- Geng, J. G.; Chen, M.; Chou, K. C. P-selectin cell adhesion molecule in inflammation, thrombosis, cancer growth and metastasis. *Curr. Med. Chem.* **2004**, *11*, 2153–2160.
- Spertini, O.; Luscinskas, F. W.; Gimbrone, M. A.; Tedder, T. F. Monocyte attachment to activated human vascular endothelium in vitro is mediated by leukocyte adhesion molecule-1 (L-selectin) under nonstatic conditions. *J. Exp. Med.* **1992**, *175*, 1789–1792.
- Kansas, G. S. Selectins and their ligands: current concepts and controversies. *Blood* **1996**, *88*, 3259–3287.
- Simanek, E.; McGarvey, G.; Jablonowski, J.; Wong, C. Selectin-carbohydrate interactions: From natural ligands to designed mimics. *Chem. Rev.* **1998**, *98*, 833–862.
- Somers, W.; Tang, J.; Shaw, G.; Camphausen, R. Insights into the molecular basis of leukocyte tethering and rolling revealed by structures of P- and E-selectin bound to SLe(X) and PSGL-1. *Cell* **2000**, *103*, 467–479.
- Berman, H.; Westbrook, J.; Feng, Z.; Gilliland, G.; Bhat, T.; Weissig, H.; Shindyalov, I.; Bourne, P. The Protein Data Bank. *Nucleic Acids Res.* **2000**, *28*, 235–242.
- Romano, S.; Slee, D. Targeting selectins for the treatment of respiratory diseases. *Curr. Opin. Invest. Drugs* **2001**, *2*, 907–913.
- Kaila, N.; Thomas, B. E. Design and synthesis of sialyl Lewis(x) mimics as E- and P-selectin inhibitors. *Med. Res. Rev.* **2002**, *22*, 566–601.
- Kaila, N.; Thomas, B. E. Selectin inhibitors. *Expert Opin. Ther. Pat.* **2003**, *13*, 305–317.
- Ohta, S.; Inujima, Y.; Abe, M.; Uosaki, Y.; Sato, S.; Miki, I. Inhibition of P-selectin specific cell adhesion by a low molecular weight, non-carbohydrate compound, KF38789. *Inflammation Res.* **2001**, *50*, 544–551.
- Thoma, G.; Kinzy, W.; Bruns, C.; Patton, J. T.; Magnani, J. L.; Banteli, R. Synthesis and biological evaluation of a potent E-selectin antagonist. *J. Med. Chem.* **1999**, *42*, 4909–4913.
- Tsai, C. Y.; Park, W. K.; Weitz-Schmidt, G.; Ernst, B.; Wong, C. H. Synthesis of sialyl Lewis X mimetics using the Ugi four-component reaction. *Bioorg. Med. Chem. Lett.* **1998**, *8*, 2333–2338.
- Beeh, K. M.; Beier, J.; Meyer, M.; Buhl, R.; Zahlten, R.; Wolff, G. Bimosiamose, an inhaled small-molecule pan-selectin antagonist, attenuates late asthmatic reactions following allergen challenge in mild asthmatics: A randomized, double-blind, placebo-controlled clinical cross-over-trial. *Pulm. Pharmacol. Ther.* **2006**, *19* (4), 233–241.
- Erbe, D. V.; Wolitzky, B. A.; Presta, L. G.; Norton, C. R.; Ramos, R. J.; Burns, D. K.; Rumberger, J. M.; Rao, B. N. N.; Foxall, C. R.; Brandley, B. H.; Lasky, L. A. Identification of an E-selectin region critical for carbohydrate recognition and cell adhesion. *J. Cell Biol.* **1992**, *119*, 215–227.
- Hiramatsu, Y.; Tsukida, T.; Nakai, Y.; Inoue, Y.; Kondo, H. Study on selectin blocker. 8. Lead discovery of a non-sugar antagonist using a 3D-pharmacophore model. *J. Med. Chem.* **2000**, *43*, 1476–1483.
- Hellwinkel, D.; Gaa, H. G.; Gottfried, R. Inverse triphenylmethylum dyes. *Z. Naturforsch.* **1986**, *B41*, 1045–1060.
- Lange, J. H. M.; Hofmeyer, L. J. F.; Hout, F. A. S.; Osnabrug, S. J. M.; Verveer, P. C.; Kruse, C. G.; Feenstra, R. W. Microwave-enhanced Goldberg reaction: a novel route to *N*-arylpiperazines and *N*-arylpiperazinediones. *Tetrahedron Lett.* **2002**, *43*, 1101–1104.
- Sapountzis, I.; Knochel, P. A new general preparation of polyfunctional diarylamines by the addition of functionalized arylmagnesium compounds to nitroarenes. *J. Am. Chem. Soc.* **2002**, *124*, 9390–9391.
- (a) Wolter, M.; Klapars, A.; Buchwald, S. L. Synthesis of *N*-aryl hydrazides by copper-catalyzed coupling of hydrazides with aryl iodides. *Org. Lett.* **2001**, *3*, 3803–3805. (b) Klapars, A.; Antilla, J. C.; Huang, X.; Buchwald, S. L. A General and efficient copper catalyst for the amidation of aryl halides and the *N*-arylation of nitrogen heterocycles. *J. Am. Chem. Soc.* **2001**, *123*, 7727–7729. (c) Kunz, K.; Scholz, U.; Ganzer, D. Renaissance of Ullmann and Goldberg reactions. Progress in copper catalyzed C–N-, C–O- and C–S-Coupling. *Synlett* **2003**, 2428–2439.
- Albright, J. D.; DeVries, V. G.; Largis, E. E.; Miner, T. G.; Reich, M. F.; Schaffer, S. A.; Shepherd, R. G.; Upešlacis, J. Potential antiatherosclerotic agents. 2. (Aralkylamino)- and (alkylamino)-benzoic acid analogues of cetaben. *J. Med. Chem.* **1983**, *26*, 1378–1393.
- Andersen, K. E.; Sørensen, J. L.; Huusfeldt, P. O.; Knutsen, L. J. S.; Lau, J.; Lundt, B. F.; Petersen, H.; Suzdak, P. D.; Swedberg, M. D. B. Synthesis of novel GABA uptake inhibitors. 4. Bioisosteric transformation and successive optimization of known GABA uptake inhibitors leading to a series of potent anticonvulsant drug candidates. *J. Med. Chem.* **1999**, *42*, 4281–4291.
- Bringmann, G.; Hartung, T.; Göbel, L.; Schupp, O.; Ewers, C. L. J.; Schöner, B.; Zagst, R.; Peters, K.; von Schnering, H. G.; Burschka, C. Synthesis and structure of benzozaphopyranones. Useful bridged model precursors for stereoselective biaryl syntheses. *Liebigs Ann. Chem.* **1992**, 225–232.
- Saez, I. M.; Mehl, G. H.; Sinn, E.; Styring, P. The effect of low molecular weight organosiloxane substituents on mesophase formation and structure in non-symmetric nickel(II) complexes. *J. Organomet. Chem.* **1998**, *551*, 299–311.
- (a) Kornet, M. J.; Thio, P. A.; Tan, S. I. The borane reduction of amido esters. *J. Org. Chem.* **1968**, *33*, 3637–3639. (b) Brown, H. C.; Heim, P. Diborane as a mild reducing agent for the conversion of primary, secondary, and tertiary amides into the corresponding amines. *J. Am. Chem. Soc.* **1964**, *86*, 3566–3567.
- (a) Jensen, A. E.; Dohle, W.; Sapountzis, I.; Lindsay, D. M.; Vu, V. A.; Knochel, P. Preparation and reactions of functionalized arylmagnesium reagents. *Synthesis* **2002**, 565–569. (b) Boudier, A.; Bromm, L. O.; Lotz, M.; Knochel, P. New applications of polyfunctional organometallic compounds in organic synthesis. *Angew. Chem., Int. Ed.* **2000**, *39*, 4414–4435. (c) Knochel, P.; Dohle, W.; Gommermann, N.; Kneisel, F. F.; Kopp, F.; Korn, T.; Sapountzis, I.; Vu, V. A. Highly functionalized organomagnesium reagents prepared through halogen–metal exchange. *Angew. Chem., Int. Ed.* **2003**, *42*, 4302–4320.
- Weitz-Schmidt, G.; Stokmaier, D.; Scheel, G.; Nifant'ev, N. E.; Tuzikov, A. B.; Bovin, N. V. An E-selectin binding assay based on a polyacrylamide-type glycoconjugate. *Anal. Biochem.* **1996**, *238*, 184–190.

- (30) Adamson, A. W.; Gast, A. P. *Physical Chemistry of Surfaces*, 6th ed.; John Wiley & Sons: New York, 1997.
- (31) Slee, D.; Romano, S.; Yu, J.; Nguyen, T.; John, J.; Raheja, N.; Axe, F.; Jones, T.; Ripka, W. Development of potent non-carbohydrate imidazole-based small molecule selectin inhibitors with antiinflammatory activity. *J. Med. Chem.* **2001**, *44*, 2094–2107.
- (32) Girard, C.; Dourlat, J.; Savarin, A.; Surcin, C.; Leue, S.; Escriou, V.; Largeau, C.; Herscovici, J.; Scherman, D. Sialyl Lewis(x) analogues based on a quinic acid scaffold as the fucose mimic. *Bioorg. Med. Chem. Lett.* **2005**, *15*, 3224–3228.
- (33) Kaila, N.; Somers, W. S.; Thomas, B. E.; Thakker, P.; Janz, K.; DeBernardo, S.; Tam, S.; Moore, W. J.; Yang, R.; Wrona, W.; Bedard, P. W.; Crommie, D.; Keith, J. C., Jr.; Tsao, D. H.; Alvarez, J. C.; Ni, H.; Marchese, E.; Patton, J. T.; Magnani, J. L.; Camphausen, R. T. Quinic acid derivatives as sialyl Lewis(x)-mimicking selectin inhibitors: design, synthesis, and crystal structure in complex with E-selectin. *J. Med. Chem.* **2005**, *48*, 4346–4357.
- (34) Ulbrich, H.; Prech, P.; Luxenburger, A.; Dannhardt, G. Nichtglykosidische und Nichtpeptidische Selektininhibitoren und Deren Verwendung (Nonglycosidic and Nonpeptidic Selectin Inhibitors and Their Uses). Dtsch. Patentanmeldung DE10 2004 036 213.0., PCT/EP2005/008125, 2004.
- (35) Bosse, R.; Vestweber, D. Only simultaneous blocking of the L- and P-selectin completely inhibits neutrophil migration into mouse peritoneum. *Eur. J. Immunol.* **1994**, *24*, 3019–3024.
- (36) Kogan, T. P.; Dupre, B.; Bui, H.; McAbee, K. L.; Kassir, J. M.; Scott, I. L.; Hu, X.; Vanderslice, P.; Beck, P. J.; Dixon, R. A. Novel synthetic inhibitors of selectin-mediated cell adhesion: synthesis of 1,6-bis[3-(3-carboxymethylphenyl)-4-(2- α -D-mannopyranosyloxy)phenyl]hexane (TBC1269). *J. Med. Chem.* **1998**, *41*, 1099–1111.
- (37) Ulbrich, H.; Prech, P.; Luxenburger, A.; Dannhardt, G. Characterization of a computerized assay for rapid and easy determination of leukocyte adhesion to endothelial cells. *Biol. Pharm. Bull.* **2005**, *28*, 718–724.
- (38) Abagyan, R. A.; Totrov, M. M.; Kuznetsov, D. A. ICM: A new method for structure modeling and design. *J. Comput. Chem.* **1994**, *15*, 488–506.
- (39) Totrov, M.; Abagyan, R. Protein–Ligand Docking as an Energy Optimization Problem. In *Drug–Receptor Thermodynamics: Introduction and Applications*; Raffa, R. B., Ed.; John Wiley & Sons: New York, 2001; pp 603–624.

JM060468Y